analytical chemistry

Article

pubs.acs.org/ac

Conformation and Dynamics of Interchain Cysteine-Linked Antibody-Drug Conjugates as Revealed by Hydrogen/Deuterium Exchange Mass Spectrometry

Lucy Yan Pan, Oscar Salas-Solano, and John F. Valliere-Douglass*

Seattle Genetics, Inc., 21823 30th Drive SE, Bothell, Washington 98021, United States

Supporting Information

ABSTRACT: Antibody-drug conjugates (ADCs) are protein therapeutics in which a target specific monoclonal antibody (mAb) is conjugated with drug molecules. The manufacturing of ADCs involves additional conjugation steps, which are carried out on the parent mAbs, and it is important to evaluate how the drug conjugation process impacts the conformation and dynamics of the mAb. Here, we present a comparative study of interchain cysteine linked IgG1 ADCs and the corresponding mAb by hydrogen/deuterium exchange mass spectrometry (HDX-MS). We found that ∼90% of the primary sequence of the ADC conjugated with either monomethyl auristatin E or F (vcMMAE/mcMMAF) displayed the same HDX kinetics as the mAb, indicating the ADCs and mAbs share very similar conformation and dynamics in solution. Minor increases in HDX kinetic rates were observed in two Fc regions in the ADCs relative to the mAb which indicated that both regions become more structurally dynamic and/or more solvent-accessible in the ADCs. The findings led to a subsequent inquiry into whether the local conformational changes were due to the presence of drugs on the interchain cysteine residues or the absence of intact interchain disulfides or both. To address this question, a side-by-side HDX comparison of ADCs, mAbs, reduced mAbs (containing 8 reduced interchain cysteine thiols), and partially reduced mAbs (conjugation process intermediate) was performed. Our results indicated that the slight increase in conformational dynamics detected at the two regions in the ADCs was due to the absence of intact interchain disulfide bonds and not the presence of vcMMAE or mcMMAF on the alkylated interchain cysteine residues. These results highlight the utility of HDX-MS for interrogating the higher-order structure of ADCs and other protein therapeutics.

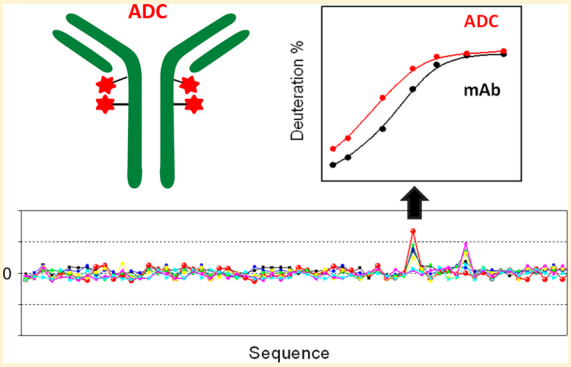

Antibody-drug conjugates (ADCs) combine the targeting specificity of a tumor-recognizing monoclonal antibody (mAb) with a small molecule drug to deliver a chemotherapeutic agent directly to cancer cells. The attachment of drugs to a targeting mAb reduces systemic toxicities to noncancerous cells that result from standard chemotherapy and also allows for the use of more potent cytotoxic agents than is possible with traditional small molecule chemotherapy.[1−3] The clinical success of ADCs is underscored by the approvals of ADCETRIS (brentuximab vedotin) for the treatment of relapsed Hodgkins lymphoma and systemic anaplastic large cell lymphoma (ALCL) and KADCYLA (ado-trastuzumab emtansine) for the treatment of HER2+ metastatic breast cancer. There are currently two dominant therapeutic modalities for ADCs: conjugation of drugs to the thiol group of cysteine residues or the epsilon amino group of lysine.[4,5] Cysteine conjugates are further classified on the basis of whether the small molecule drug is attached to endogenous-reduced interchain cysteine residues[6] or to cysteines that are specifically engineered into the primary sequence for site-directed conjugation.[7,8] Conjugation to interchain cysteines can selectively generate an ADC with a heterogeneous composition of drugs per mAb varying from 0 to 8.[6] Lysine-linked ADCs are generated by conjugating drugs to lysine residues in mAbs with a covalent linker and generally also result in a heterogeneous distribution of drugs per mAb.[9,10] Lysine conjugates also have considerable added complexity relative to interchain cysteine conjugates, because of the large number of lysine residues in primary sequence that are subject to conjugation.[11]

In the development of ADC modalities, the choice of drug-linkers, the site of incorporation, and the conjugation process itself may have unforeseen impacts on the structure and function of ADCs. ADCs are intrinsically more complex and heterogeneous than mAbs.[12] The complexity of ADCs has highlighted the need for analytical approaches aimed at gaining a better understanding of the relevant quality attributes.[13,14] There are several approaches described in the literature that have focused on adapting techniques used to assess the quality attributes of mAbs and applying these techniques to ADCs. Considerable work has also gone into defining unique methods to answer key questions specific to ADCs such as drug loading and distribution.[15−17] The primary benefit of assessing a mAb

Received: December 10, 2013
Accepted: February 11, 2014
Published: February 11, 2014

and the corresponding ADC using the same method is that side by side analytical comparisons of the mAb and ADC highlight key quality attributes that are impacted by conjugation of the mAb with drug molecules.

There is also a growing emphasis on developing techniques and approaches that can be applied to proteins to gain a better understanding of higher-order structure. This is particularly important for protein-based therapeutics, because the mode of action can be affected by aberrant changes in the higher-order structure or structural dynamics of the therapeutics. The term higher-order structure is commonly used to refer to protein conformation. It is generally understood that a protein must fold into a specific conformation to be functional. At the same time, proteins in solution are known to be highly dynamic and protein dynamics is also closely associated with protein function and stability.[18,19] The manufacturing of ADCs involves additional processing steps during conjugation, and it is important to evaluate how the drug conjugation process impacts the conformation and dynamics of the mAb intermediate. NMR and X-ray crystallography are high-resolution techniques that provide insights into protein conformation; however, the size (~150 kDa) and heterogeneity of mAbs and ADCs make these high-resolution techniques unsuitable for routine application. Traditional biophysical techniques such as circular dichroism (CD), fluorescence, and differential scanning calorimetry (DSC) are typically employed[20−22] for assessing protein higher-order structure but the information that can be obtained from these techniques, while useful, is limited. CD can provide information on protein secondary structural elements such as α-helical and β-sheet content, as well as conformational stability in response to stress conditions.[23,24] However, the data represent an average across the sequence of the protein and an average of protein conformers present in the sample and thus provides little local, detailed structural information. Ionescu et al. have previously shown that DSC can be used to provide insight into the domain specific stability of mAbs[20] and Wakankar et al. have demonstrated that the ADC (TDM-1) has a less stable C_H2 domain, compared the corresponding mAb by DSC.[22] Nevertheless, similar to CD, DSC cannot resolve local structural perturbations. Furthermore, observed differences in stability at temperatures in excess of 60 °C may not have real-world implications for stability, because they are considerably higher than storage, shipping, and in vivo conditions in which the molecule will be exposed to.

Hydrogen/deuterium exchange mass spectrometry (HDX-MS) has emerged as an important approach for understanding the conformation and dynamics of protein therapeutics in solution.[25−32] HDX-MS involves assessing the rates of exchange of protein backbone amide hydrogens in the presence of D_2O under native conditions. The specific exchange of hydrogen for deuterium causes an increase in the mass of the protein analyte, which can be monitored and quantitated by mass spectrometry. The rate and extent of deuterium incorporation depends on the solvent accessibility and hydrogen bonding of the individual backbone amides and can vary as much as 10^8, depending on the conformation and dynamics of the protein.[33] When coupled with enzymatic digestion, structurally resolved information on the conformational properties of proteins can be obtained at the peptide level. This technique has been successfully applied to the detection of domain specific conformational changes in mAbs induced by post-translational modifications (PTMs) and chemical modifications,[34,35,29] comparisons of the conformation and stability of mAb acidic variants,[36] and to investigate mechanisms of mAb aggregation.[37,38] The capacity of HDX-MS to monitor conformational changes at the peptide level makes the technique well-suited for providing detailed insights into the impact of drug conjugation processes on the higher-order structure of mAbs.

This report seeks to address the domain specific changes in mAb conformation and dynamics that occur as a consequence of conjugating humanized IgG1 antibodies with vcMMAE or mcMMAF drugs following partial reduction of interchain disulfide bonds. The understanding of ADC conformation and dynamics gained by implementation of comparative HDX-MS demonstrates the importance of this approach in the development of ADCs and other protein therapeutics.

MATERIAL AND METHODS

Materials. Pepsin from porcine stomach mucosa, sodium phosphate, sodium chloride, urea, formic acid, tris(2-carboxyethyl)phosphine HCl (TCEP), dithiothreitol (DTT), and ethylenediamine tetraacetic acid (EDTA) were purchased from Sigma (St. Louis, MO). Deuterium oxide (D_2O) was obtained from Cambridge Isotope Laboratories (Andover, MA). NAP-5 columns were from GE Healthcare. All chemicals were used as received. mAb-A and mAb-B are humanized IgG1 kappa monoclonal antibodies expressed in Chinese hamster ovary cells. mAb-A intermediate was conjugated with valine-citrulline-monomethyl auristatin E (vcMMAE) and mAb-B intermediate was conjugated with maleimidocaproyl-monomethyl Auristatin F (mcMMAF) to form the vcMMAE and mcMMAF ADCs, respectively. The ADCs and mAbs were produced at Seattle Genetics using established procedures.[12] Partially reduced mAb-A or mAb-B (containing an average of four reduced interchain cysteine thiols) was prepared by incubating the mAb in 2.2 mol equiv TCEP and 5 mM EDTA for 100 min. Fully reduced mAb-A or mAb-B (containing 0 interchain disulfide bonds) was prepared by incubating the mAb in 10 mM DTT (final concentration) for 30 min.

HIC Chromatography. The vcMMAE and mcMMAF ADCs were separated on the basis of drug loading by HIC as previously described.[39] Briefly, a 4.6 mm × 35 mm Butyl-NPR column (Tosoh, Japan) was used to separate discrete drug-loaded forms of the vcMMAE ADC and a 4.6 mm × 100 mm column was used to separate the mcMMAF ADC. The HIC separation was carried out by binding the ADC to the stationary phase in the presence of 25 mM (mcMMAF) or 50 mM (vcMMAE) sodium phosphate pH 7.0, 1.5 M ammonium sulfate. The ADC samples were eluted from the stationary phase with a linear gradient to the buffer B mobile phase; 25 mM (mcMMAF) or 50 mM (vcMMAE) sodium phosphate pH 7.0, 25% isopropanol (v:v). Discrete drug-loaded species were quantitated and expressed as an average molar ratio of drug to antibody (MR_D) by integrating the UV area of each species at 280 nm.

Native SEC-MS. Intact mass determination of ADCs was carried out by previously described online SEC-MS procedures.[39] Briefly, ADCs were deglycosylated by adding 1 μL of PNGase F per 100 μg of ADC and incubating at 37 °C for 4 h. Subsequently 40 μg ADC samples were desalted with a 2.1 mm × 200 mm polyhydroxyethyl-A (PHEA) column (PolyLC, Columbia, MD) containing 5 μm particles with 300 Å pores. The column was pre-equilibrated in 200 mM ammonium acetate at an unadjusted pH of ~7. The column was directly

dx.doi.org/10.1021/ac404003q | Anal. Chem. 2014, 86, 2657−2664

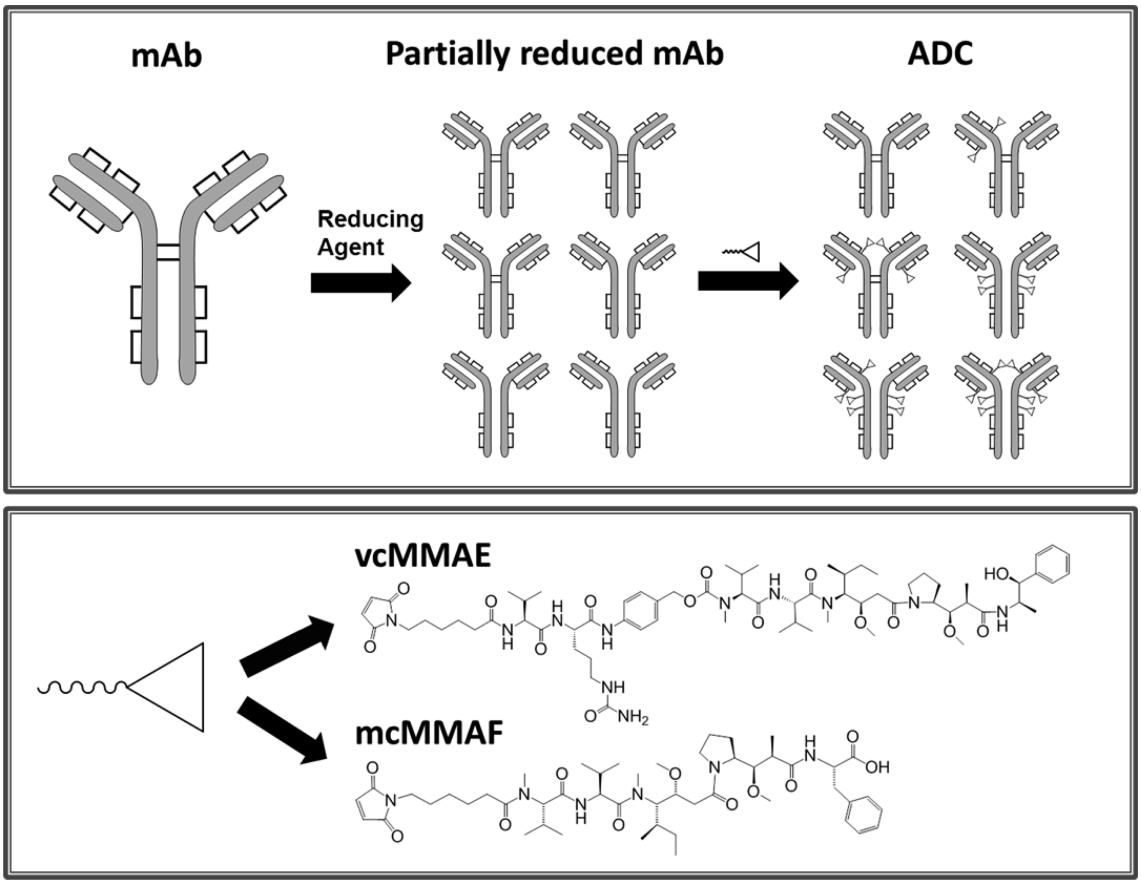

Figure 1. ADCs are manufactured by partially reducing mAb interchain disulfide bonds and adding maleimidyl drug linkers, which alkylate the reduced interchain cysteine residues (top panel). The chemical structures of vcMMAE and mcMMAF drug linkers are shown in the bottom panel.

coupled to an Agilent 6510 QTOF (Agilent, Santa Clara, CA) operated in positive electrospray ionization (ESI) mode within the range of 1000−8000 m/z. The raw data was converted to zero charge mass spectra using a maximum entropy deconvolution algorithm within the MassHunter workstation software version B.03.01.

Hydrogen/Deuterium Exchange Mass Spectrometry. Prior to HDX experiments, all protein samples (mAb, ADC, partially reduced and fully reduced mAb) were buffer-exchanged into the labeling buffer (50 mM sodium phosphate, 100 mM sodium chloride, pH 7.0) using NAP-5 columns. Deuterium labeling was initiated at room temperature by mixing 100 μL of protein samples (10 mg/mL) with 900 μL of D_2O-based labeling buffer (50 mM sodium phosphate and 100 mM sodium chloride, pH 7.0). After various labeling times ranging from 30 s to 22 h, 50-μL aliquots were removed and mixed with 50 μL of quenching buffer (210 mM TCEP, 7.4 M urea, pH 2.5), followed by flash freezing in liquid nitrogen. Prior to LC/MS analysis, the quenched samples were thawed and digested by adding 50 μL of a pepsin stock solution (3 mg/mL, pH 4.5) for a final pH of 2.5 and incubating for 6 min on ice. Fifty microliters (50 μL) of the resulting digests were loaded into a Waters BEH C8 column (2.1 mm × 50 mm) held at 0 °C. To minimize back exchange, the column, accessories, injector, and solvent delivery lines were submerged in an ice bath. Chromatographic separations were carried out at a flow rate of 90 μL/min. Solvent A was 0.1% aqueous formic acid, and solvent B was acetonitrile with 0.1% formic acid.

Mass spectrometry measurements were performed on a Q-Exactive high-resolution mass spectrometer (Thermo Scientific, San Jose, CA). Peptide spectra were acquired in positive ion mode with a resolution of 70 000 (at m/z 400). Identification of the peptides was performed by tandem mass spectroscopy (MS/MS) in a data-dependent acquisition mode. Peptide identity was confirmed using SEQUEST score, isotopic pattern, and exact mass. No adjustment was made for deuterium back exchange, and all results are reported as the relative deuteration level. The relative deuteration percent of individual peptides was determined as follows:

$$\text{Deuteration}\,(\%) = \frac{m - m_0}{N - 2 - N_p} \times 100 \quad (1)$$

where m and m_0 are the centroid mass value of the labeled and unlabeled peptide, respectively. N is the number of residues of the peptide, and N_p is the number of proline residues that are not located in the first two positions of the peptide. It is assumed that the first two residues of any peptide will not retain any deuterium after HPLC separation, because of their rapid back exchange.[40] HDExaminer data analysis software (Sierra Analytics) was employed to calculate the centroid mass of each peptide as a function of labeling time. The mass difference (ΔD) of individual peptides between ADC and mAb was determined as

$$\Delta D = m_{\text{ADC}} - m_{\text{mAb}} \quad (2)$$

where m_{ADC} and m_{mAb} are the centroid mass of the same peptide from the ADC and the mAb, respectively.

dx.doi.org/10.1021/ac404003q | Anal. Chem. 2014, 86, 2657−2664

RESULTS AND DISCUSSION

Characterization of ADC by HIC and SEC-MS. The manufacturing of interchain cysteine linked vcMMAE or mcMMAF ADCs consists of two steps, which are illustrated in Figure 1. The first step involves a partial reduction of interchain disulfide bonds of the IgG1 under native conditions, generating a conjugation process intermediate that contains an average of 2 interchain disulfides and 4 free thiol groups per mAb. The second step involves alkylation of the thiol groups with vcMMAE or mcMMAF drug linkers. The conjugation scheme results in a heterogeneous ADC containing a distribution of 0−8 drugs per mAb. The extent of reduction is controlled so that an average of 4 drug molecules per mAb are covalently linked to interchain cysteine residues. It is an established practice to use HIC to determine drug loading for vcMMAE and mcMMAF ADCs, and the separation of differentially loaded species into individual peaks is well-documented.[13,14,17,41] The vcMMAE ADC was analyzed by HIC to determine the molar ratio of drugs to antibody (MR_D) and by SEC-MS to confirm molar mass of discrete drug loaded forms of the ADC (see Figures 2A and 2B, respectively). The

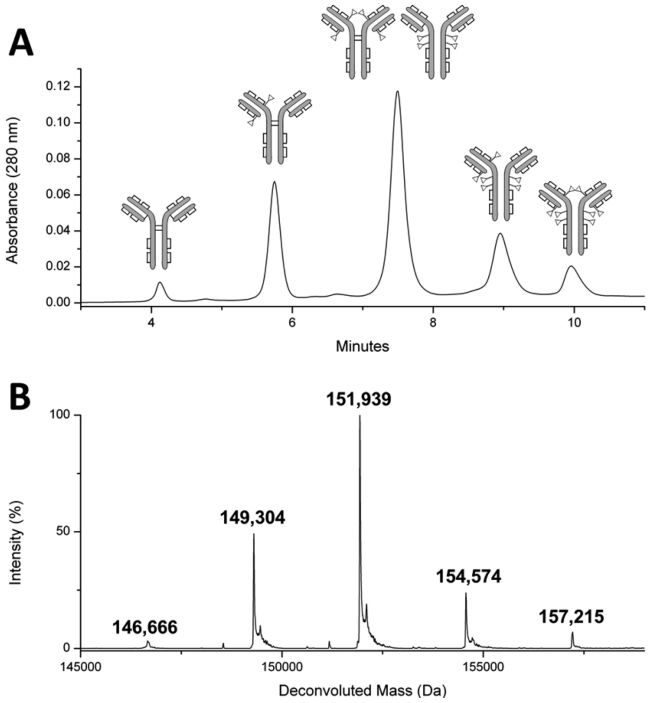

Figure 2. Characterization of vcMMAE ADC by HIC and SEC-MS: (A) HIC separation of the vcMMAE ADC showing the distribution of individually loaded forms, and (B) deconvoluted mass spectra for the deglycosylated vcMMAE ADC. The five different mass values correspond to five ADC subpopulations with 0, 2, 4, 6, or 8 drugs per mAb, respectively.

measured MR_D value was 4.1 as targeted, and a qualitative evaluation of the HIC profile indicated that there was no evidence of unfolded species or dissociated heavy chains and light chains. The mcMMAF ADC was analyzed in the same way, and similar results were observed (data not shown). The partially reduced mAb-A and mAb-B were also tested by SEC-MS. SEC-MS comparison of mAb-B and partially reduced mAb-B are shown in the Supporting Information (Figure S1). The deconvoluted masses of intact mAb and partially reduced mAb confirm that the partially reduced mAb remained associated as noncovalent complexes consisting of 2 heavy chains and 2 light chains under native conditions, despite the partial loss of interchain disulfide bonds.

HDX-MS Analysis of mAb-A and vcMMAE ADC. The vcMMAE ADC and mAb-A were incubated in D_2O buffer under the exact same conditions (the same pH, temperature, buffer, etc.). The extent of deuterium uptake was assessed over 7 time points (from 0.5 min to 22 h) by quenching the sample with acidic buffer and digesting with pepsin as described in the Material and Methods section. In-solution pepsin digestion was employed here for better sequence coverage and lower peptide carry-over between runs. Approximately 100 peptic peptides were identified that were common in the mAb and ADC and also had isotopic profiles that could be monitored during HDX labeling experiments. Approximately 95% of the amino acid sequence was recovered as peptic fragments with the exception of the heavy-chain hinge region and the N-linked glycopeptide. It is worth noting that all peptides identified in the mAb can be detected in the ADC with the only difference being that the ADCs also contain some substoichiometric levels of drug-linked peptides. For the purposes of this comparative study, we only focused on non-drug-linked peptides, because they have identical primary sequences and chemical compositions in mAbs and ADCs and, thus, are directly comparable by HDX.

Consistent with the approaches described in previous reports,[42] mirror (butterfly) plots were employed to illustrate the HDX behavior of the vcMMAE ADC and mAb-A. The HDX kinetics of 54 individual peptides were defined as the relative deuteration percent of the peptide as a function of the labeling time and are shown in Figure 3A. These peptides consist of contiguous light-chain and heavy-chain amino acid sequence and cover 94% of the total mAb sequence. The HDX rates of the individual peptides provide a structural fingerprint for the whole mAb or ADC and, in general, the HDX profiles of the mAb and ADC are very similar. For purposes of comparing the mAb to the ADC, the mass difference (ΔD) of the individual peptides at each time point was determined as shown in eq 2. Similar to previous reports,[42] we found that the error associated with mass measurement was in the absolute range of 0.05−0.15 Da for each data point based on three repeated injections with our system. We thus concluded that reproducible changes in mass greater than ±0.5 Da were significant and a threshold of ±0.5 Da was adopted for purpose of assessing similarity. If the mass difference of a peptide from two samples is greater than 0.5 Da, the difference is due to different deuterium incorporation levels, not measurement errors. It is apparent, from the plot of ΔD shown in Figure 3B, that there is a high degree of similarity between the ADC and mAb. For each time point, the ΔD of 52 peptides covering ∼90% sequence is within ±0.2 Da which indicates that the mAb and ADC exhibit the same HDX behavior over that sequence. There are only two peptides, H244−255 (heavy chain peptide from 244 to 255) and H337−351 (heavy-chain peptide from 337 to 351), which have ΔD values at or just above the significance threshold for some time points. H244−255 and H337−351 have positive ΔD values, indicating that the ADC peptides displayed increased deuterium uptake relative to mAb peptides and, thus, are more structurally dynamic and/or more solvent-accessible in the ADC.

The slightly different deuterium uptake observed in the Fc domain of the ADC relative to the mAb prompted a follow-up investigation into whether the difference was due to

dx.doi.org/10.1021/ac404003q | Anal. Chem. 2014, 86, 2657−2664

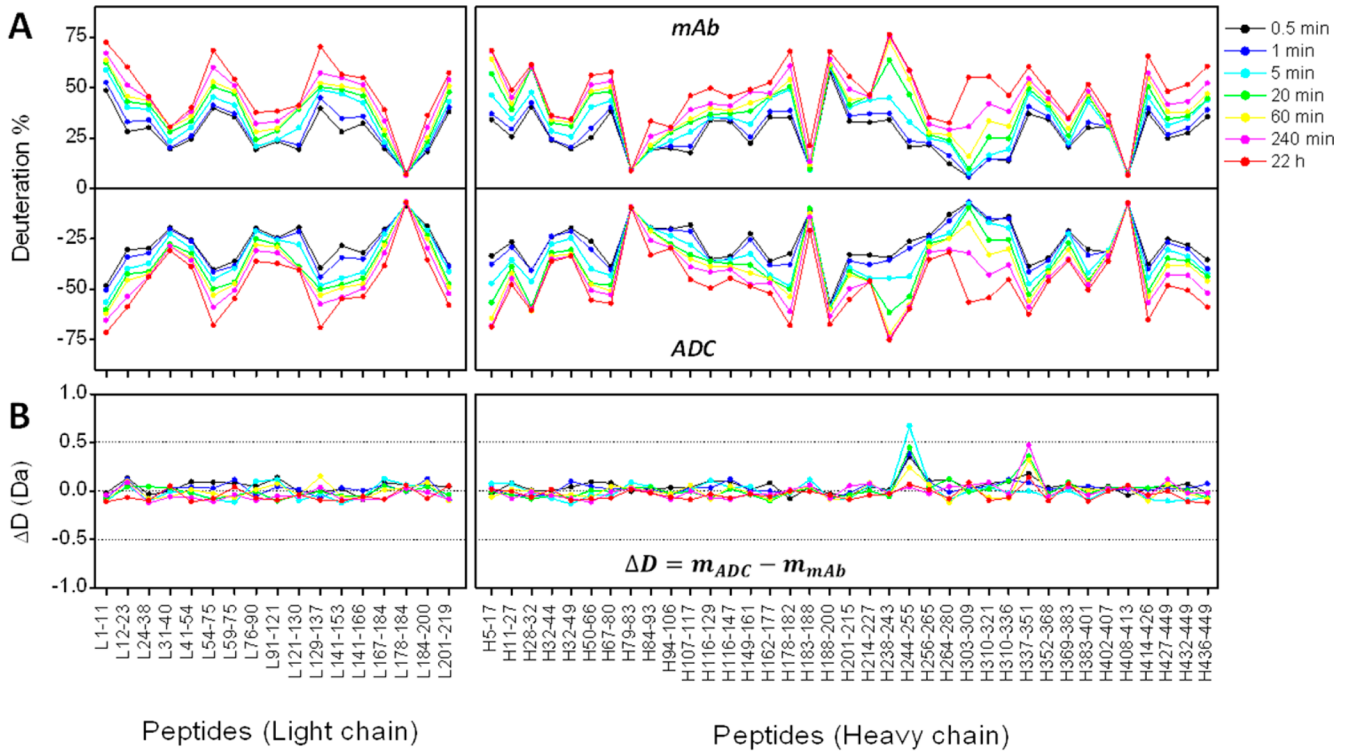

Figure 3. HDX comparison of the vcMMAE ADC and corresponding mAb-A. (A) Mirror plot of the HDX kinetics of mAb-A (top), versus the vcMMAE ADC (bottom). The *x*-axis is the position of individual peptides. Heavy-chain and light-chain peptides are designated as H or L, respectively, followed by the numerical position of the peptide in the linear amino acid sequence. The *y*-axis is the deuteration percent of individual peptides calculated by eq 1. The black, blue, light blue, green, yellow, magenta, and red lines correspond to data acquired at 0.5, 1, 5, 20, 60, 240 min, and 22 h of deuterium labeling, respectively, for both samples. Each data point is an average of two or three experiments and the standard deviation is ≤2%. Error bars are not shown. (B) Mass difference (ΔD) plot of individual peptides from the vcMMAE ADC and mAb-A at each labeling time point. ΔD was calculated using eq 2 from the average data shown in Figure 3A. The dotted lines at *y*-axis values of ±0.5 Da represent the threshold for identifying significant differences between the mAb and ADC peptides.

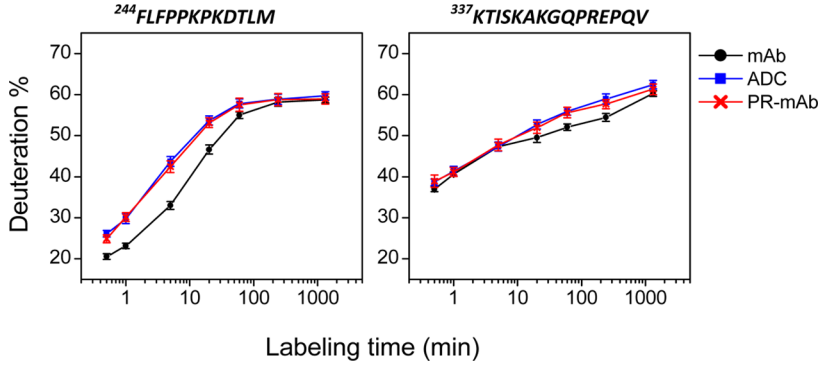

Figure 4. Comparison of the HDX kinetics for two peptides FLFPPKPKDTLM (C_H2 domain, left) and KTISKAKGQPREPQV (C_H2-C_H3 interface, right) in different samples: mAb-A (black line and data points), vcMMAE ADC (blue line and data points), and partially reduced mAb-A (red line and data points).

interactions between the vcMMAE drug and the mAb or the absence of interchain disulfides in a subpopulation of the ADC. To understand the consequences of reduction of interchain disulfide bonds on the conformational properties of IgG1, mAb-A was treated with TCEP under native conditions to partially reduce an average of 2 interchain disulfide bonds (yielding ∼4 reduced interchain thiols), followed by deuterium labeling. For the sake of consistency, the same 54 peptides were monitored for the partially reduced mAb-A, as were monitored in the comparison of vcMMAE ADC and intact mAb-A. The results from the comparison of the mAb and the partially reduced mAb indicated that there was no significant difference in deuterium uptake in 52 out of 54 peptides. Similar to the results from the ADC, however, two heavy-chain peptides, H244−255 (residues: FLFPPKPKDTLM) and H337−351 (residues: KTISKAKGQPREPQV) in the Fc domain of partially reduced mAb-A, exhibited increased HDX kinetics (see Figure 4). The relative increase in exchange kinetics for the two peptides in the partially reduced mAb was similar in magnitude to the increased exchange kinetics observed for the same peptides in the ADC. It thus follows that intact interchain disulfides reduce conformational dynamics of local protein

dx.doi.org/10.1021/ac404003q | *Anal. Chem.* 2014, 86, 2657−2664

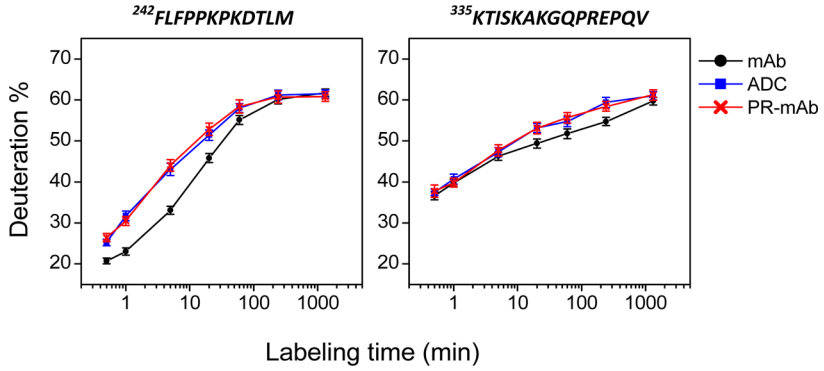

Figure 5. Comparison of the HDX kinetics for two peptides FLFPPKPKDTLM (C_H2 domain, left) and KTISKAKGQPREPQV (C_H2–C_H3 interface, right) in different samples: mAb-B (black line and data points), mcMMAF ADC (blue line and data points), and partially reduced mAb-B (red line and data points).

domains in the C_H2 and C_H2–C_H3 interface of IgG1 mAbs but leave the Fab domains unchanged. Subsequent HDX experiments on fully reduced mAb-A showed that the complete elimination of interchain disulfide bonds resulted in larger increases in the HDX kinetics of H244–255 and H337–351, compared to the partially reduced mAb-A and the vcMMAE ADC (data not shown), further confirming the role of interchain disulfides on the conformation and dynamics of the Fc domain of IgG1 antibodies.

HDX-MS Analysis of mAb-B and mcMMAF ADC. To determine if the results observed for the vcMMAE ADC were generalizable to other drug linkers, an interchain cysteine linked mcMMAF ADC, mAb-B and partially and fully reduced mAb-B were also analyzed by HDX. As was the case for vcMMAE ADC, the mcMMAF ADC and partially reduced mAb-B displayed a high degree of similarity to nonreduced mAb-B throughout 90% of the amino acid sequence. Also consistent with the experiments on vcMMAE ADC, local increases in the HDX kinetics of the C_H2 and C_H2–C_H3 interface peptides, H242–253 (residues: FLFPPKPKDTLM) and H335–349 (residues: KTISKAKGQPREPQV) were observed in the mcMMAF ADC and partially reduced mAb-B as compared to the nonreduced mAb-B (see Figure 5). Note that the length of CDR-H3 (in the Fab) is different in mAb-A versus mAb-B, which results in different sequential numbering in the Fc domain for the same amino acid sequences. Similar to the vcMMAE ADC/mAb-A system, full reduction of all interchain disulfides on mAb-B resulted in relatively higher increases in deuterium uptake at the two regions described above, compared to the mcMMAF ADC and partially reduced mAb-B (data not shown). Overall, the results on the mcMMAF ADC/mAb-B system recapitulated the findings from the vcMMAE ADC/mAb-A system and supported the conclusion that minor local conformational changes observed in the Fc domain of vcMMAE or mcMMAF ADCs are due to the absence of intact interchain disulfide bonds. Furthermore, our results were consistent with orthogonal analyses of mAb and ADC structure by DSC in which it has been reported that the ADC has lower melting temperature for the C_H2 and C_H3 domains, relative to the mAb.[43]

Impact of Drug Linker on mAb Conformation and Dynamics. Since the constant domains of mAb-A and mAb-B are identical and comprise over 70% of the amino acid sequence, it is expected then that the Fc domains of mAb-A and mAb-B would display very similar HDX behavior. Comparing the exchange kinetics shown in Figure 4 with that shown in Figure 5, it is apparent that the two regions (FLFPPKPKDTLM and KTISKAKGQPREPQV) in the Fc domain exhibited almost identical HDX kinetics in the mAb-A and mAb-B. More importantly, the two regions also show very similar HDX profiles in vcMMAE and mcMMAF ADCs. This suggests that, despite the chemical differences between vcMMAE and mcMMAF drug molecules, both have no observable impact on the conformation and dynamics of the partially reduced mAb. It is unclear at this point whether the nonimpact of drug linkers on a higher-order structure is a universal feature of interchain cysteine conjugated ADCs, regardless of drug linker chemotype. Additional HDX-MS studies on ADCs with other chemotypes could shed light on this question.

Modeling IgG1 Fc Domain Structural Motifs. In order to understand the spatial relationship of the two regions in Fc domain that were observed to be more structurally dynamic in ADCs and partially reduced mAbs, we highlighted the corresponding C_H2 and C_H2–C_H3 interface regions in the crystal structure of the model IgG1 (PDB: 1HZH)[44] in Figure 6. It should be noted that the sequences of Fc domains of mAb-A and mAb-B are identical to the model IgG1, 1HZH. The peptic peptide in the C_H2 domain (FLFPPKPKDTLM), highlighted in red color, starts as a β-strand and extends to a short α-helix in the lower part of the C_H2 domain. This region is proximally adjacent to the other peptic peptide described above (KTISKAKGQPREPQV), which is highlighted in blue color and spans the C_H2 and C_H3 domains. Based on the crystal structure 1HZH shown in Figure 6, both regions are significantly spatially separated from the interchain disulfide bonds in the IgG1 mAb, which indicates that the conformational changes in the two areas observed in ADC are unlikely to be caused by direct interactions with drug molecules, which are attached at the interchain cysteine residues in the hinge and Fab region.

The interchain disulfide bond structure of IgG1 molecules is highly conserved through evolution and plays an important role in stabilizing the IgG1 molecule structure. The HDX data on two partially reduced IgG1s (mAb-A and mAb-B) indicates that the reduction of an average of 2 interchain disulfide bonds will not cause significantly different HDX kinetics in the Fab domain, but will induce increased deuterium uptake in specific C_H2 and C_H2–C_H3 interface peptides. Consistent with this result, ADCs lacking the same site specific proportion of interchain disulfide bonds due to drug occupancy at the interchain cysteine residues also display increased deuterium

dx.doi.org/10.1021/ac404003q | Anal. Chem. 2014, 86, 2657–2664

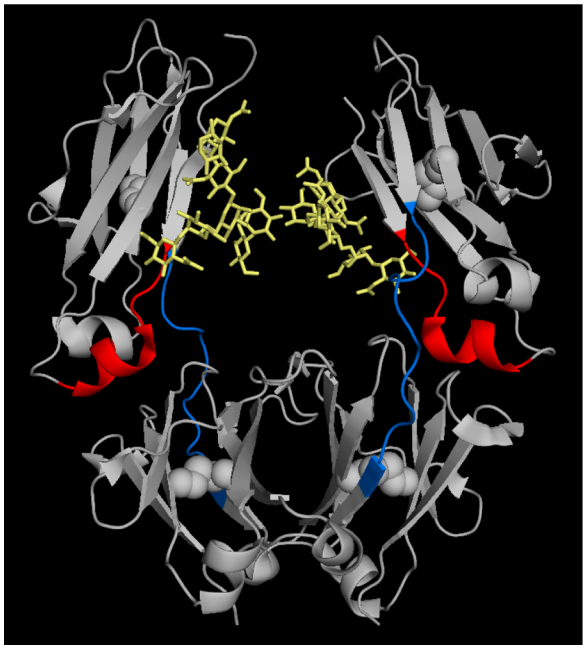

Figure 6. Crystal structure of the Fc domain of a humanized IgG1 (PDB: 1HZH). Residues of the C_H2 domain peptide FLFPPKPKDTLM and the C_H2–C_H3 interface peptide KTISKAKGQPREPQV that exhibit increased HDX in ADCs and partially/fully reduced mAbs, relative to the intact mAbs, are highlighted in red and blue, respectively. Glycans are depicted as yellow sticks and the four intrachain disulfides are depicted as spheres.

uptake at the same C_H2 and C_H2–C_H3 interface peptides. It is not known at this time if the minor differences observed between mAbs and the corresponding ADCs are directly relevant to the stability of the molecules under physiological conditions.

CONCLUSIONS

This work represents the first application of HDX-MS to the direct comparison of mAbs and the corresponding ADCs for the specific purpose of understanding the impact of drug conjugation on the conformation and dynamics of ADCs. The HDX kinetics of ADCs with vcMMAE or mcMMAF drug linkers were assessed over seven time-points spanning 0.5 min to 22 h and compared to the same dataset from intact, as well as partially and fully reduced mAbs. Taken together, the HDX-MS data indicate that the conformational properties of vcMMAE or mcMMAF ADCs and the corresponding mAbs are very similar across a 90% amino acid sequence, demonstrating the drug conjugation process described here does not induce large-scale conformational changes on the protein backbone. Only two local regions, located within the C_H2 domain and the C_H2 and C_H2–C_H3 interface, respectively, become slightly more structurally dynamic and/or solvent exposed as a consequence of drug conjugation. In subsequent HDX studies on the partially reduced mAbs (conjugation process intermediates), we found that the observed minor local conformational changes are due to the partial loss of interchain disulfide bonds in ADCs. In addition, the presence of vcMMAE and mcMMAF drug molecules at interchain cysteine residues does not further impact the conformation of the partially reduced mAb in any significant manner. Our results demonstrate the great potential of HDX-MS to broaden our understanding of higher-order structures in ADCs and other protein therapeutics.

ASSOCIATED CONTENT

Supporting Information

This material is available free of charge via the Internet at http://pubs.acs.org.

AUTHOR INFORMATION

Corresponding Author

*E-mail: jdouglass@seagen.com.

Author Contributions

The manuscript was written through contributions of all authors. All authors have given approval to the final version of the manuscript.

Notes

The authors declare no competing financial interest.

ABBREVIATIONS

ADC = antibody-drug conjugate
HDX-MS = hydrogen–deuterium exchange mass spectrometry
vcMMAE = valine-citrulline-monomethyl auristatin E
mcMMAF = maleimidocaproyl-monomethyl Auristatin F
mAb = monoclonal antibody
ALCL = anaplastic large cell lymphoma
NMR = nuclear magnetic resonance
CD = circular dichroism
DSC = differential scanning calorimetry
IgG = Immunoglobulin G
Fc = fragment crystallizable
Fab = fragment antigen-binding
CDR = complementarity determining region
LC/MS = liquid chromatography mass spectrometry
SEC-MS = size exclusive chromatography mass spectrometry
HIC = hydrophobic interaction chromatography

REFERENCES

(1) Alley, S. C.; Zhang, X.; Okeley, N. M.; Anderson, M.; Law, C. L.; Senter, P. D.; Benjamin, D. R. *J. Pharmacol. Exp. Ther.* **2009**, *330*, 932–938.
(2) Ikeda, H.; Hideshima, T.; Fulciniti, M.; Lutz, R. J.; Yasui, H.; Okawa, Y.; Kiziltepe, T.; Vallet, S.; Pozzi, S.; Santo, L.; Perrone, G.; Tai, Y. T.; Cirstea, D.; Raje, N. S.; Uherek, C.; Dalken, B.; Aigner, S.; Osterroth, F.; Munshi, N.; Richardson, P.; Anderson, K. C. *Clin. Cancer Res.* **2009**, *15*, 4028–4037.
(3) Lutz, R. J.; Whiteman, K. R. *MAbs* **2009**, *1*, 548–551.
(4) Adair, J. R.; Howard, P. W.; Hartley, J. A.; Williams, D. G.; Chester, K. A. *Expert Opin. Biol. Ther.* **2012**, *12*, 1191–1206.
(5) Sievers, E. L.; Senter, P. D. *Annu. Rev. Med.* **2012**, *64*, 15–29.
(6) Doronina, S. O.; Toki, B. E.; Torgov, M. Y.; Mendelsohn, B. A.; Cerveny, C. G.; Chace, D. F.; DeBlanc, R. L.; Gearing, R. P.; Bovee, T. D.; Siegall, C. B.; Francisco, J. A.; Wahl, A. F.; Meyer, D. L.; Senter, P. D. *Nat. Biotechnol.* **2003**, *21*, 778–784.
(7) Junutula, J. R.; Bhakta, S.; Raab, H.; Ervin, K. E.; Eigenbrot, C.; Vandlen, R.; Scheller, R. H.; Lowman, H. B. *J. Immunol. Methods* **2008**, *332*, 41–52.
(8) Kung Sutherland, M. S.; Walter, R. B.; Jeffrey, S. C.; Burke, P. J.; Yu, C.; Kostner, H.; Stone, I.; Ryan, M. C.; Sussman, D.; Lyon, R. P.; Zeng, W.; Harrington, K. H.; Klussman, K.; Westendorf, L.; Meyer, D.; Bernstein, I. D.; Senter, P. D.; Benjamin, D. R.; Drachman, J. G.; McEarchern, J. A. *Blood* **2013**, *122*, 1455–1463.
(9) Hamann, P. R.; Hinman, L. M.; Hollander, I.; Beyer, C. F.; Lindh, D.; Holcomb, R.; Hallett, W.; Tsou, H. R.; Upeslacis, J.; Shochat, D.;

Mountain, A.; Flowers, D. A.; Bernstein, I. *Bioconjug. Chem.* **2002**, *13*, 47−58.
(10) Blanc, V.; Bousseau, A.; Caron, A.; Carrez, C.; Lutz, R. J.; Lambert, J. M. *Clin. Cancer Res.* **2011**, *17*, 6448−6458.
(11) Wang, L.; Amphlett, G.; Blattler, W. A.; Lambert, J. M.; Zhang, W. *Protein Sci.* **2005**, *14*, 2436−2446.
(12) Sun, M. M.; Beam, K. S.; Cerveny, C. G.; Hamblett, K. J.; Blackmore, R. S.; Torgov, M. Y.; Handley, F. G.; Ihle, N. C.; Senter, P. D.; Alley, S. C. *Bioconjug. Chem.* **2005**, *16*, 1282−1290.
(13) Wakankar, A.; Chen, Y.; Gokarn, Y.; Jacobson, F. S. *MAbs* **2011**, *3*, 161−172.
(14) Alley, S. C.; Anderson, K. E. *Curr. Opin. Chem. Biol.* **2013**, *17*, 406−411.
(15) Valliere-Douglass, J. F.; McFee, W. A.; Salas-Solano, O. *Anal. Chem. 84*, 2843−2849.
(16) Xu, K.; Liu, L.; Saad, O. M.; Baudys, J.; Williams, L.; Leipold, D.; Shen, B.; Raab, H.; Junutula, J. R.; Kim, A.; Kaur, S. *Anal. Biochem.* **2011**, *412*, 56−66.
(17) Chen, J.; Yin, S.; Wu, Y.; Ouyang, J. *Anal. Chem.* **2013**, *85*, 1699−1704.
(18) Henzler-Wildman, K.; Kern, D. *Nature* **2007**, *450*, 964−972.
(19) Bhabha, G.; Lee, J.; Ekiert, D. C.; Gam, J.; Wilson, I. A.; Dyson, H. J.; Benkovic, S. J.; Wright, P. E. *Science* **2011**, *332*, 234−238.
(20) Ionescu, R. M.; Vlasak, J.; Price, C.; Kirchmeier, M. *J. Pharm. Sci.* **2008**, *97*, 1414−1426.
(21) Hawe, A.; Kasper, J. C.; Friess, W.; Jiskoot, W. *Eur J. Pharm. Sci.* **2009**, *38*, 79−87.
(22) Wakankar, A. A.; Feeney, M. B.; Rivera, J.; Chen, Y.; Kim, M.; Sharma, V. K.; Wang, Y. J. *Bioconjug. Chem.* **2010**, *21*, 1588−1595.
(23) Vermeer, A. W.; Norde, W. *Biophys. J.* **2000**, *78*, 394−404.
(24) Graef, R. R.; Anderson, G. P.; Doyle, K. A.; Zabetakis, D.; Sutton, F. N.; Liu, J. L.; Serrano-Gonzalez, J.; Goldman, E. R.; Cooper, L. A. *BMC Biotechnol.* **2011**, *11*, 86.
(25) Engen, J. R. *Anal. Chem.* **2009**, *81*, 7870−7875.
(26) Houde, D.; Arndt, J.; Domeier, W.; Berkowitz, S.; Engen, J. R. *Anal. Chem.* **2009**, *81*, 2644−2651.
(27) Kaltashov, I. A.; Bobst, C. E.; Abzalimov, R. R. *Anal. Chem.* **2009**, *81*, 7892−7899.
(28) Kaltashov, I. A.; Bobst, C. E.; Abzalimov, R. R.; Berkowitz, S. A.; Houde, D. *J. Am. Soc. Mass Spectrom.* **2009**, *21*, 323−337.
(29) Houde, D.; Peng, Y.; Berkowitz, S. A.; Engen, J. R. *Mol. Cell. Proteomics* **2010**, *9*, 1716−1728.
(30) Bobst, C. E.; Kaltashov, I. A. *Curr. Pharm. Biotechnol.* **2011**, *12*, 1517−1529.
(31) Kaltashov, I. A.; Bobst, C. E.; Abzalimov, R. R.; Wang, G.; Baykal, B.; Wang, S. *Biotechnol. Adv.* **2011**, *30*, 210−222.
(32) Kaltashov, I. A.; Bobst, C. E.; Abzalimov, R. R. *Protein Sci.* **2013**, *22*, 530−544.
(33) Smith, D. L.; Deng, Y.; Zhang, Z. *J. Mass Spectrom.* **1997**, *32*, 135−146.
(34) Bobst, C. E.; Abzalimov, R. R.; Houde, D.; Kloczewiak, M.; Mhatre, R.; Berkowitz, S. A.; Kaltashov, I. A. *Anal. Chem.* **2008**, *80*, 7473−7481.
(35) Burkitt, W.; Domann, P.; O'Connor, G. *Protein Sci.* **2010**, *19*, 826−835.
(36) Tang, L.; Sundaram, S.; Zhang, J.; Carlson, P.; Matathia, A.; Parekh, B.; Zhou, Q.; Hsieh, M. C. *MAbs* **2012**, *5*, 114−125.
(37) Zhang, A.; Qi, W.; Singh, S. K.; Fernandez, E. J. *Pharm. Res.* **2011**, *28*, 1179−1193.
(38) Zhang, A.; Singh, S. K.; Shirts, M. R.; Kumar, S.; Fernandez, E. J. *Pharm. Res.* **2011**, *29*, 236−250.
(39) Valliere-Douglass, J. F.; McFee, W. A.; Salas-Solano, O. *Anal. Chem.* **2012**, *84*, 2843−2849.
(40) Bai, Y.; Milne, J. S.; Mayne, L.; Englander, S. W. *Proteins* **1993**, *17*, 75−86.
(41) Xu, K.; Liu, L.; Dere, R.; Mai, E.; Erickson, R.; Hendricks, A.; Lin, K.; Junutula, J. R.; Kaur, S. *Bioanalysis* **2013**, *5*, 1057−1071.
(42) Houde, D.; Berkowitz, S. A.; Engen, J. R. *J. Pharm. Sci.* **2011**, *100*, 2071−2086.
(43) Guo, J.; Kumar, S.; Prashad, A.; Starkey, J.; Singh, S. K. *Pharm. Res.* **2014**, in press (DOI: 10.1007/s11095-013-1274-2).
(44) Saphire, E. O.; Parren, P. W.; Pantophlet, R.; Zwick, M. B.; Morris, G. M.; Rudd, P. M.; Dwek, R. A.; Stanfield, R. L.; Burton, D. R.; Wilson, I. A. *Science* **2001**, *293*, 1155−1159.